Molecules and Cells

Research article

Biallelic variants of *SEMA3F* are associated with nonsyndromic hearing loss

Sun Young Joo[1,2,†], Hyehyun Min[3,†], Jung Ah Kim[1,2], Se Jin Kim[1,2], Seung Hyun Jang[1,2], Ho Lee[4], Kyu Min Kim[2,5], Je Kyung Seong[5], Jae Young Choi[2,6], Jinsei Jung[2,6,*], Jinwoong Bok[2,3,*], and Heon Yung Gee[1,2,7,*]

[1]Department of Pharmacology, Brain Korea 21 PLUS Project for Medical Sciences, Yonsei University College of Medicine, Seoul 03722, Republic of Korea, [2]Won Sang Institute for Hearing Loss, Seoul 03722, Republic of Korea, [3]Department of Anatomy, Brain Korea 21 PLUS Project for Medical Sciences, Yonsei University College of Medicine, Seoul 03722, Republic of Korea, [4]Graduate School of Cancer Science and Policy, National Cancer Center, Goyang-si 10408, Republic of Korea, [5]Laboratory of Developmental Biology and Genomics, BK21 PLUS Program for Creative Veterinary Science Research, Research Institute for Veterinary Science, College of Veterinary Medicine, Seoul National University, Seoul 08826, Republic of Korea, [6]Department of Otorhinolaryngology, Yonsei University College of Medicine, Seoul 03722, Republic of Korea, [7]Woo Choo Lee Institute for Precision Drug Development, Seoul 03722, Republic of Korea

*Correspondence: jsjung@yuhs.ac (J. Jung), bokj@yuhs.ac (J. Bok), hygee@yuhs.ac (H.Y. Gee).

https://doi.org/10.1016/j.mocell.2025.100190

ABSTRACT

It is crucial to manage hearing loss and its associated public health impacts. In this study, we aimed to understand the role of Sema3f in the development and maintenance of the auditory system. Inner ear-specific *Sema3f* knockout mice exhibited hearing loss at 8 weeks with an elevated threshold for auditory brainstem response and an absent threshold for distortion product optoacoustic emission tests. Additionally, an increased number of outer hair cells and abnormal patterns of spiral ganglion neuron projections in the outer hair cell regions were observed. Through the analyses of sequencing data from 558 families with hearing loss, we identified biallelic variants of *SEMA3F*, which encodes semaphorin-3F, in one of the families. In the family, the proband showed profound progressive nonsyndromic hearing loss with congenital onset. In vitro analysis revealed that the identified missense variants decreased the furin-mediated processing of SEMA3F and abolished the cellular abilities of SEMA3F, which collapsed the filamentous actin cytoskeleton in human umbilical vein-derived endothelial cells. Our data suggest that *SEMA3F* is essential for normal hearing and is associated with nonsyndromic hearing loss in humans.

Keywords: Exome sequencing, Hearing loss, Outer hair cell, SEMA3F, Spiral ganglion neuron

INTRODUCTION

Hearing loss is a common sensory disorder characterized by genetic heterogeneity. More than 125 genes have been associated with nonsyndromic hearing loss (Jang et al., 2024; Shearer et al., 1993; Zhong et al., 2013). Although many genes are linked to hearing loss, genetic testing on 1,119 patients with hearing loss showed a diagnostic rate of approximately 39%, which suggests that the genetic causes of approximately half of the hereditary hearing loss cases were still undefined and exceptionally rare (Sloan-Heggen et al., 2016). Identification of additional associations of genes to hearing loss is needed to fill the diagnostic gap. Mouse deafness genes are excellent representations of human deafness genes (Kikkawa et al., 2012). Two notable studies on mouse phenotyping suggested 329 deafness genes to date, which contained 69 orthologs for human deafness genes (Bowl et al., 2017; Ingham et al., 2019).

As one of the 329 mouse deafness genes, *SEMA3F* (MIM: 601124) encodes semaphorin-3F, which is an essential protein for the proper innervation of spiral ganglion neurons (SGNs) within the hair cells of the cochlea (Coate et al., 2015). Semaphorin-3F functions as a repulsive cue, mediating SGNs to avoid extension into the outer hair cell (OHC) region, thereby ensuring correct connection to the inner hair cells (IHCs). In *Sema3f* knockout mice, this guidance is disrupted, resulting in an increased number of neuronal fibers within the OHC region.

Abbreviations: *Sema3f* cKO, *Sema3f* conditional knockout; OTO, osmium tetroxide/thiocarbohydrazide; TBCT, temporal bone computed tomograms

† These authors contributed equally to this work.

eISSN: 1016-8478

These mice also exhibited significantly elevated auditory brainstem response (ABR) thresholds, particularly at low frequencies, highlighting the essential role of *SEMA3F* in auditory function.

Despite the established role of *SEMA3F* in the mouse auditory system, evidence linking it to human deafness remains unclear. *SEMA3F* has not been functionally validated as a human disease gene, and it is not listed on the Online Mendelian Inheritance in Man database. Previous mouse phenotyping studies have suggested that *Sema3f* is involved in several biological processes, including auditory function. Mice systemically lacking *Sema3f* not only display hearing loss but also present with multiple syndromic phenotypes, such as cataracts, an increased startle reflex, and preweaning lethality. This raises the question of whether the hearing loss observed in the knockout mice was due to defects specifically within the inner ear or to other systemic abnormalities.

The aim of this study was to investigate the cellular basis of hearing loss in *Sema3f*-deficient mice using *Sema3f* conditional knockout (Sema3f cKO) mice with inner ear-specific deletion. Our objectives included characterizing cochlear defects leading to hearing loss in these mice. Additionally, we aimed to identify genetic variants of *SEMA3F* associated with nonsyndromic hearing loss in humans by sequencing data from 558 individuals, pinpointing biallelic missense variants in 1 family. Furthermore, we aimed to conduct in vitro analyses to confirm the functional consequences of these variants, establishing them as loss-of-function mutations. Overall, our study highlights SEMA3F as a critical gene for hearing function in both mice and humans, contributing to our understanding of genetic mechanisms underlying genetic hearing loss.

MATERIALS AND METHODS

Animals

C57BL/6N-Sema3f$^{tm1c(EUCOMM)Hmgu/}$*H* mice were purchased from the European Mouse Mutant Archive (catalog # 09031) and designated as *Sema3f*$^{fl/fl}$. Inner ear-specific *Sema3f* conditional knockout (*Sema3f* cKO) mice were generated by crossing *Sema3f*$^{fl/fl}$ mice with *Pax2-Cre* transgenic mice (Ohyama and Groves, 2004). The *Pax2-Cre* line was obtained from the Mutant Mouse Resource and Research Center (stock #, 010569-UNC). The animal protocol was approved by the Institutional Animal Care and Use Committee of Yonsei University College of Medicine (approved number: 2022-0330).

Scanning Electron Microscopy (SEM)

Samples were prepared for SEM analysis as described previously (Son et al., 2015). We dissected inner ears of 8-week-old *Sema3f* cKO mice and fixed in 2% paraformaldehyde. We separated tectorial membrane and the cochlear epithelium and fixed 15 h at 4°C. The fixed samples were washed thrice, dehydrated, dried, fixed on a stub, and coated (ACE600, Leica Microsystems). By using a Schottky microscope, the specimens were imaged after being mounted (JSM-IT500).

Immunoblotting and Immunofluorescence

We conducted the assays as previously described (Koh et al., 2022; Park et al., 2025). Antibodies we used in this study were anti-SEMA3F (NBP1-90665; Novus Biologicals), anti-paxillin (ab32084; Abcam), anti-GAPDH (sc-20357), anti-NF200 (N0142; Sigma-Aldrich), and anti-CtBP2 (BS2287; Bioworld) antibodies and Alexa-linked phalloidin (Invitrogen). In every immunoblotting analysis, we used primary antibodies and the corresponding anti-isotype secondary antibodies (Santa Cruz Biotechnology) diluted with a ratio of 1:1,000 and at a 1:2,000 dilution, respectively. We used a SuperSignal West-Pico kit (Thermo Fisher Scientific) to visualize signals. Immunofluorescence was assayed in human umbilical vein-derived endothelial cells using blocking buffer. The inner ears dissected from P0 and 3-week-old *Sema3* cKO mice were fixed in 4% paraformaldehyde in PBS at 4°C for 10 min and 1 h, respectively. The permeabilization of the cochleae was performed with 0.5% Triton-X 100. We obtained and processed confocal images using Carl Zeiss microscopes (Carl Zeiss) and ZEN software (Carl Zeiss).

Auditory Brainstem Response

ABR was measured as previously described (Ma et al., 2022). As briefly mentioned, we performed the ABR threshold tests in a chamber with soundproof walls using Tucker-Davis Technologies (TDT) and BioSigRZ software. Using SigGenRZ software, we measured either a click- or tone-burst stimuli at varying thresholds, including 4, 6, 8, 10, 12, 18, 24, 30, and 42 kHz. Electrodes were placed on the right and left ears and at the vertex of the anesthetized mice. The ABR signals were input into a low-impedance Medusa Biological Amplifier System (RA4LI, TDT), which then relayed the signal to the RZ6 digital signal-processing hardware. The recorded signals were filtered through a 0.5 to 1 kHz band-pass filter, and the ABR waveforms were averaged based on responses to 512 tone bursts. Peak amplitudes (mV) and latencies (ms) were derived from the waveform signal of the click-evoked ABRs.

Distortion Product Otoacoustic Emission

The distortion product otoacoustic emission (DPOAE) was measured at 6, 8, 10, 12, 16, 18, 24, and 30 kHz utilizing a TDT microphone-speaker system. We determined the DPOAE input/output at 6 and 30 kHz with a frequency ratio (f2/f1) of 1.2 and equal intensity levels (L1 = L2). The intensity level of the primary tones was increased from 20 to 80 decibels sound pressure level (dB SPL) in 5 dB SPL increments. Fast Fourier transform was performed for each primary tone to obtain distortion product (DP) grams and at each intensity for the input/output functions using BioSigRZ software, determining the average spectra of the 2 primaries, 2f1-f2 distortion products, and noise floors.

Statistical Analysis

With at least 3 times of experiments, statistical analyses to compare the 2 groups were carried out using Student's t-tests or 2-way analysis of variance (2-way ANOVA), incorporating Bonferroni corrections for multiple comparisons. We used 2-sided *P*-values and considered the tests with the corrected

P-values below .05 as significant. GraphPad Prism 8.0 software (GraphPad Software) was used for the statistical analyses.

Gene Ontology Enrichment Analysis

Gene ontology (GO) enrichment analyses were performed using enrichGO in ClusterProfiler (v4.0, R package) (Chua et al., 2024; Kim et al., 2022; Wu et al., 2021). To investigate the functional similarity of genes involved in hearing in humans and mice, 188 genes linked to syndromic or nonsyndromic hearing loss in humans from the Hereditary Hearing Loss database (http://hereditaryhearingloss.com/, May 1, 2024, Table S1), and 329 genes linked to an increased ABR threshold in mice were retrieved from the International Mouse Phenotyping Consortium (https://www.mousephenotype.org/), Mouse Genome Informatics (http://www.informatics.jax.org/), and review of literatures (Table S2) (Bowl et al., 2017; Ingham et al., 2019). Fifteen markedly enriched GO terms from the analysis of human and mouse deafness genes were compared.

Research Subjects

This study received approval from the institutional review board of Severance Hospital, Yonsei University Health System (IRB #4-2015-0659). Informed written consent was secured from participants with hearing loss for both their involvement in the study and the publication of their clinical data. Enrollment in the Yonsei University Hearing Loss (YUHL) cohort was based on the stringent criterion of having hearing loss unassociated with congenital cytomegalovirus infection or any other medical conditions that are clinically possible to affect auditory function. We prescreened for pathogenic biallelic variants in *SLC26A4* and *GJB2* or copy number variations (CNVs) in *STRC*, which are the most common genetic causes in East Asians (Jung et al., 2017; Kim et al., 2020). In total, probands from 437 families with no pathogenic variants of these 3 known genes were included in the cohort for exome sequencing; the majority had nonsyndromic hearing loss.

Subject Evaluation

We obtained audiograms for patients and their family members. We measured thresholds of bone conduction (250-4,000 Hz). Pure-tone air (250-8,000 Hz) thresholds were also derived using the same protocol. We averaged thresholds at 500, 1,000, 2,000, and 4,000 Hz and determined final thresholds. We also measured steady-state auditory in infants. We conducted temporal bone computed tomograms and magnetic resonance imaging to check for inner ear abnormalities.

Variant Calling

Genomic DNA was extracted from the blood or saliva samples of 558 patients. A TruSeq DNA Nano Library Prep Kit (Illumina, Inc) was used to prepare sequencing libraries. For germline variant calling, we designed a sequence analysis pipeline following the GATK best practices. FASTQ files generated on the Novaseq platform (Illumina) were aligned to the hg19 reference using the BWA mem aligner v0.7.17 (Li, 2013). Following the marking of duplicates and coordinate sorting with MarkDuplicates, the mapping quality was recalibrated using Base Quality Score Recalibration, as implemented in GATK version 4.1.9.0 (Van der Auwera et al., 2013). Single nucleotide variants (SNVs) and small indels were subsequently identified using GATK HaplotypeCaller with the option "-ERCGVCF" (Poplin et al., 2017). To detect CNV in exome-sequencing data, we utilized EXCAVATOR2 (D'Aurizio et al., 2016) and ExomeDepth version 1.1.16 (Plagnol et al., 2012) and merged overlapping regions to analyze CNV. For calling CNV in whole-genome sequencing (WGS) data, the GATK-SV pipeline, a structural variation discovery pipeline for Illumina short-read WGS data (Collins et al., 2021), was used for the analysis.

Evaluation of Pathogenic Variants

First, we evaluated whole-exome or genome sequencing data from 558 families, specifically targeting deleterious variants in 188 known hearing loss genes (Chang et al., 2015; Rim et al., 2022; Shin et al., 2019; Yu et al., 2019). If no known causality was identified, the filtering process was performed based on pedigree and a suspected disease inheritance mode. This included a filtering step based on allele frequency in a public population database (gnomAD) and the evolutionary conservation of amino acids (Oh et al., 2023; Rim et al., 2019). The remaining variants were ranked on the basis of 5 in silico prediction scores provided by PolyPhen-2, SIFT, Mutation Taster, CADD, and Condel and then prioritized. Final candidate genes were identified by a panel of otolaryngologists and geneticists. We confirmed whether the causative variants were segregated within families whenever familial DNA (from parents or siblings) was available.

Plasmid Construction

We purchased human *SEMA3F* complementary DNA from OriGene Technologies. The full-length *SEMA3F* was subcloned into the pcDNA6.2-EmGFP vector (Invitrogen) using LR Clonase (Invitrogen). We used a Quick Change II XL site-directed mutagenesis kit (Agilent Technologies) to create the *SEMA3F* variant.

Cell Culture and Transfection

We cultured human embryonic kidney 293 transformed (HEK293T) cells in Dulbecco's modified essential medium supplemented with 10% fetal bovine serum and penicillin (50 IU/ml) or streptomycin (50 μg/ml, Invitrogen). We used Transporter 5 as a transfection reagent (Polysciences) according to the manufacturer's instructions. HUVECs were cultured on gelatin-coated dishes in a conditioned medium (ScienCell Research Laboratories).

Endothelial Contraction Assay

Endothelial contraction assays were performed as described previously (Guttmann-Raviv et al., 2007). Briefly, HEK293T cells were transfected with plasmids carrying wild-type and variant SEMA3F in serum-free media. After 72 h of incubation, the culture medium was collected, concentrated using Amicon Ultra-4 (Millipore), and used for immunoblotting or treatment of HUVECs seeded in 48-well plates (2×10^4 cells/well).

RESULTS

In Vivo Analysis on Mice With Inner Ear-Specific Deletion of *Sema3F*

Previous studies have reported that the systematic deletion of *Sema3f* in mice causes a significantly lower live-birth rate (5.7%-14.0%) than the expected Mendelian ratio, suggesting a semilethal phenotype (Regano et al., 2017; Walz et al., 2007). Therefore, we generated a *Sema3f* cKO by crossing *Pax2-Cre* and *Sema3f*$^{fl/fl}$ mice. *Sema3f* cKO mice survived until adulthood, but were smaller in size, exhibiting significantly lower body weights than wild-type (*Sema3f*$^{fl/fl}$) or *Pax2-Cre;Sema3f*$^{fl/+}$ (*Sema3f* HET) mice at 8 weeks (Fig. 1A). To examine the hearing sensitivity of *Sema3f* cKO mice, we measured the ABR evoked by click stimuli of mixed broadband (2-4 kHz) or pure-tone sounds at individual frequencies at 8 weeks (Fig. 1B). Nine of the 13 *Sema3f* cKO mice exhibited a considerably high ABR threshold at all frequencies, except 42 kHz (filled red circles, n = 9/12), whereas the remaining 4 mice showed a slightly higher ABR threshold at 4 to 8 kHz than that of the 9 mice, which was only significant at 4 kHz (empty red circles, n = 3/12). *Sema3f* HET mice exhibited normal ABR threshold at any frequency (blue circles, n = 6) compared with wild-type mice (*Sema3f*$^{fl/fl}$, black circles, n = 13). Moreover, the input/output ABR amplitude functions evoked by click stimuli were significantly lower at all sound intensities in *Sema3f* cKO mice than that in wild-type mice (Fig. 1B), suggesting that the firing ability of auditory nerve fibers induced by IHCs was impaired in the absence of SEMA3F function.

Next, we examined whether OHC function was also impaired in *Sema3f* cKO mice by measuring the DPOAE thresholds at 8 weeks (Fig. 1B). Consistent with the ABR threshold (Fig. 1B), DPOAE thresholds were significantly higher at all frequencies, except 30 kHz in 9 of the 12 *Sema3f* cKO mice, which exhibited increased ABR thresholds, but not in the other 4 *Sema3f* cKO or *Sema3f* HET mice compared with the wild-type mice (Fig. 1B). Moreover, the input/output DPOAE amplitude functions of *Sema3f* cKO mice exhibiting elevated ABR thresholds were significantly reduced at 6 and 30 kHz (Fig. 1B).

To examine hair cell and stereociliary bundle morphology, immunofluorescence and SEM analyses were performed at postnatal day (P) 0 (Fig. 1C) and 8 weeks (Fig. 1D), respectively. At P0, the basal cochlea within the organ of Corti in Sema3f cKO mice displayed no discernible defects in either organization or morphology, appearing completely normal. However, an extra row of OHCs was observed in the apical cochlea (Fig. 1C and D). The number of OHCs was significantly higher in the apical cochlea of *Sema3f* cKO mice than that in wild-type mice but not in the middle or basal cochlea (Fig. 1C and F; n = 4 for *Sema3f* cKO and n = 3 for wild-type). In 8-week-old *Sema3f* cKO mice, an extra row of OHCs was observed (Fig. 1D and F). In contrast, the stereociliary bundles of IHCs were lost in the apical, but not in the middle and basal cochlear regions (Fig. 1D; yellow arrowheads), with a significant difference (Fig. 1F; n = 3).

A previous study showed that systematic *Sema3f* deletion increases the number of SGN projections to the OHC region, suggesting that SEMA3F normally acts as a repulsive signal preventing SGN fibers from extending into the OHC domain (Coate et al., 2015). Similar results were observed in *Sema3f* cKO mice with an increased number of SGN processes in the OHC region stained using anti-NF200 antibodies (Fig. 1E). Furthermore, we found that the SGN processes, which normally project into the OHC domain and turn toward the base to form 3 parallel rows in wild-type mice (Fig. 1E), often turned in the opposite direction and appeared to be greatly disorganized in *Sema3f* cKO mice (Fig. 1E; white arrowhead). Unlike the increased number of SGN nerve processes, the number of ribbon synapses stained with anti-CiBP2 antibodies in OHCs and IHCs did not differ significantly between *Sema3f* cKO and wild-type mouse cochleas (Fig. 1F). Taken together, these results indicate that SEMA3F is required for normal hearing by mediating multiple functions during cochlear development, including the regulation of OHC numbers, IHC stereociliary maintenance, and SGN projections.

WES Analysis Identified Missense Variants of *SEMA3F*

We also identified a patient with *SEMA3F* variants in the YUHL cohort (Jung et al., 2024; Oh et al., 2023). The cohort consisted of 558 probands whose WES or WGS data were generated and analyzed to identify pathogenic variants in molecular genetic testing. After the evaluation of rare variants in the known deafness genes, 371 patients (66% of the cohort) with hereditary hearing loss carried no causative variants in 188 deafness genes. Based on pedigree information, we searched for genes with potentially deleterious variants or combinations (in a recessive pedigree) by prioritizing genes with minor allele frequencies in gnomAD and the Korean Variant Archive 2, in silico scores, and mouse deafness genes (Fig. 2). We included mouse deafness genes to prioritize candidate genes based on a GO analysis. When comparing the 15 most enriched GO terms, biological processes related to hearing in humans and mice were similar (Fig. S1). In addition, mouse deafness genes suggested a gene set that is implicated in mouse deafness, but not in humans, such as neuronal development (Fig. S1). Given the similarities in their biological processes, mouse deafness genes are excellent candidate genes for studying hearing loss in humans.

Of the 558 patients, one proband in a Korean family diagnosed with profound congenital progressive nonsyndromic hearing loss was identified to be compound heterozygous for 2 missense variants in *SEMA3F* (NM_004186: c.1123T > C, p.Ser375Pro and NM_004186: c.2061C > A, p.His687Gln; Fig. 3A and Table 1). Analysis of the patient's WES data did not reveal pathogenic variants, including CNV in any of the genes previously associated with hearing loss (Fig. 2). Sanger sequencing showed that the p.His687Gln variant of *SEMA3F* was inherited from the unaffected mother and the p.Ser375Pro variant of *SEMA3F* was inherited from the affected father with mild hearing loss that developed in his 30s and a pure-tone auditory (PTA) threshold of 36 and 38 dB in the left and right ears, respectively (Figs. 3B and S2). The patient with compound heterozygous variants of *SEMA3F* had no inner ear abnormalities, as observed by temporal bone imaging, including temporal bone computed tomograms and magnetic resonance imaging, and no transient-evoked otoacoustic emission

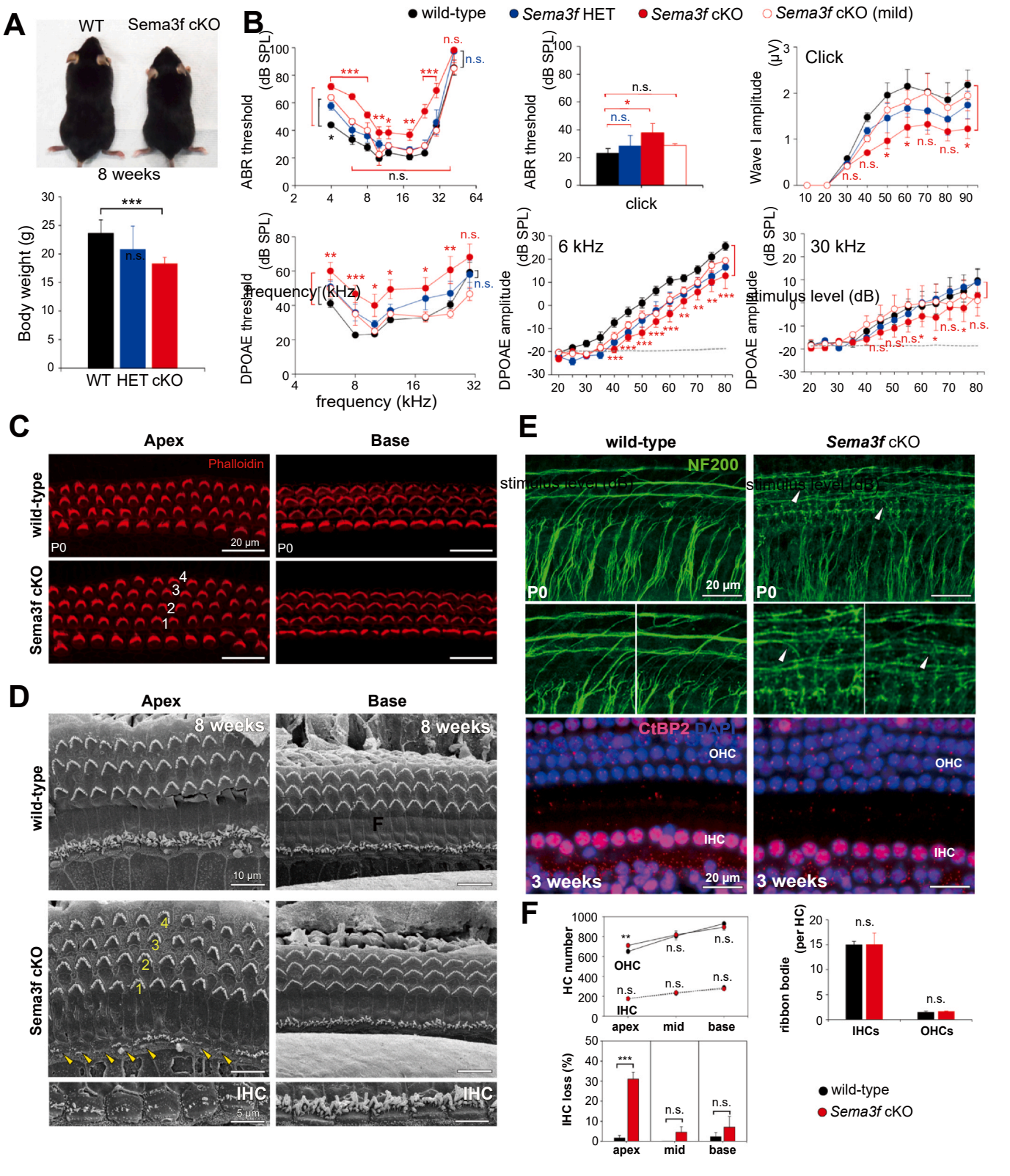

(caption on next page)

Fig. 1. *SEMA3F* is required for normal hearing in mice. (A) Overall appearances and body weight of *Sema3f* cKO mice, HET, and wild-type mice at 8 weeks of age. (B) Tone-pip ABR thresholds, click ABR thresholds, ABR input/output functions, DPOAE thresholds, and DPOAE input/output functions in *Sema3f* cKOs with hearing loss (filled red circles, $n = 9/12$), *Sema3f* cKOs with mild hearing loss (empty red circles, $n = 3/12$), *Sema3f* HET mice (blue circles, $n = 6$), and wild-type mice (black circles, $n = 13$) at 8 weeks. Data represent the mean ± SEM. (C) Immunofluorescence images of the organ of Corti stained with phalloidin in P0 *Sema3f* cKO and wild-type mice displaying an extra row of OHCs at the apex. Scale bars = 20 μm. (D) SEM images of 8-week-old *Sema3f* cKO and wild-type mice showing stereocilia of OHCs and IHC in the apex. Scale bars in (A)-(D) 10 μm, (E)-(F) 5 μm. (E) SGN processes stained with anti-NF200 antibodies in wild-type and *Sema3f* cKO mice at P0. Disorganized SGN projections into the OHC domain in *Sema3f* cKOs indicated in arrowheads. Ribbon synapses and nuclei in auditory hair cells are stained with anti-CtBP2 antibodies and DAPI, respectively, at 3 weeks. Scale bars in (A)-(D) 20 μm. (F) OHC number and IHC loss in the apex of *Sema3f* cKOs and wild-type mice. The number of ribbon synapses between wild-type and *Sema3f* cKO mice. Statistical comparisons are performed using 2-way ANOVA with Bonferroni's correction for multiple comparisons (*$P < .05$, **$P < .01$, ***$P < .001$). n.s., nonsignificant.

response. A PTA threshold of 85 dB was measured in the right ear, whereas the left ear showed no response at any frequencies.

SEMA3F is a secretory protein that consists of a SEMA domain, which is involved in dimerization and binding to receptor plexins or neuropilins, an immunoglobulin (Ig) domain, a plexin-semaphorin-integrin domain, and a basic tail (Fig. 3C) (Toledano et al., 2019). The identified variants were located in 2 different domains. The p.Ser375Pro variant in the SEMA domain affected an evolutionarily conserved residue and was observed in only 3 of the 1,461,780 alleles in gnomAD v4 (allele frequency: 0.000002052; Fig. 3C and Table 1). Alphamissense, an effective tool for predicting the pathogenicity of single amino-acid changes, predicted the variant to be pathogenic (Fig. 3C) (Cheng et al., 2023). In contrast, the p.His687Gln variant of SEMA3F was in the Ig domain and was predicted by Alphamissense to have an ambiguous effect on the protein structure (Fig. 3C). The p.His687Gln variant was not present in the gnomAD database (Table 1). Both variants were absent from the Korean Variant Archive 2, which consists of 5,305 healthy Korean individuals (Lee et al., 2022).

In Vitro Analysis Revealed Loss-of-Function Effect of *SEMA3F* Variants

To assess the functional effects of p.Ser375Pro and p.His687Gln variants, we first examined the expression of wild-type and variant proteins in the lysates and media. SEMA3F is a homodimeric protein (Toledano et al., 2019) consisting of identical monomers. Cells overexpressing the *SEMA3F* p.Ser375Pro variant showed a significant decrease in the dimerized forms of full-length SEMA3F (approximately 181 kDa) or processed SEMA3F (approximately 137 kDa) in both lysates and media (Fig. 4A; both $P < .05$). The monomeric forms of SEMA3F were significantly increased in cell lysates expressing the p.Ser375Pro variant. This was probably due to the failure of the proteins to form dimer complexes. In contrast, the p.His687Gln variant showed no difference in the expression of monomeric and dimeric forms of SEMA3F in the lysates (Fig. 4A). Interestingly, the processed form of secreted SEMA3F, a cleavage product of furin protease (22 kDa), was significantly reduced in both variants (Fig. 4A; $P < .001$, $P < .05$). The reduced dimerized SEMA3F subsequently leads to a decrease in the processed forms of the p.Ser375Pro variant protein. However, how the p.His687Gln variant results in decreased proteolytic processing remains unresolved.

Furin processing in the C-terminal region of SEMA3F is important for producing a mature protein that is essential for effective binding to neuropilins (Parker et al., 2010). By binding to the canonical receptor complex, SEMA3F mediates multiple signaling pathways and cellular events (Bielenberg et al., 2004) such as filamentous actin cytoskeleton collapse, characterized by the loss of stress fibers and focal contact (Bielenberg et al., 2008). To examine whether the variant proteins affected cellular functions in vitro, HUVECs were chosen because of their expression of neuropilin-2 (NRP2), which acts as a functional receptor for SEMA3F (Shimizu et al., 2008). HUVECs were suspended in the supernatants of cells overexpressing wild-type SEMA3F, variant SEMA3F protein carrying p.Ser375Pro or p.His687Gln, and seeded on a 6-well plate coated with gelatin. When HUVECs were treated with wild-type SEMA3F, a similar pattern of actin disorganization was observed as that of the positive control (one treated with latrunculin B for disrupting microfilament organization) (Fig. 4B). However, these morphological changes were not observed in HUVECs suspended in the supernatants of either SEMA3F variant protein, suggesting that the variants led to the loss of function of wild-type SEMA3F (Fig. 4B).

DISCUSSION

In the present study, we performed functional studies on *SEMA3F* in vivo. Studies on *Sema3f* cKO mice with inner ear-specific deletion of *Sema3f* have shown that the hearing loss in the homozygous *Sema3f* cKO mice phenocopied with global KO mice with multiple abnormalities in the cochlea. Abnormal numbers of OHCs and increased SGN projections were detected in the region of OHCs, suggesting that the loss of *Sema3f* causes deficits in the axon guidance of sensory neurons in the *Sema3f* cKO mice. These results indicate a distinctive role of Sema3f in the inner ear development involved in SGN innervation and pruning.

In this study, we provided the first evidence linking *SEMA3F* to hearing loss in humans. Biallelic missense variants of *SEMA3F* were identified in a proband of the YUHL120 family with nonsyndromic, profound, and congenital hearing loss. The 2 SEMA3F proteins from cells expressing each of the missense variants failed to collapse the cytoskeletal filamentous actin structures of HUVECs, unlike the wild-type SEMA3F. In addition, we identified a decrease in the processed form of the secreted SEMA3F protein. Furin is a cellular endoprotease that proteolytically activates several proprotein substrates. *SEMA3F*

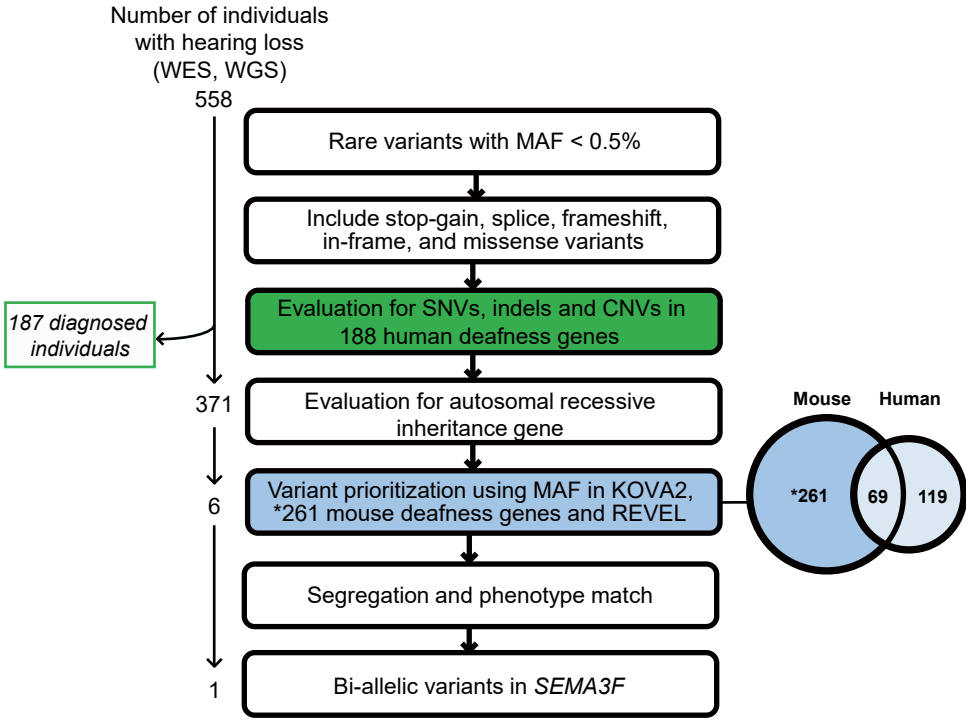

Fig. 2. Filtering criteria utilized in the identification of human *SEMA3F* variants. We perform candidate gene discovery for individuals molecularly undiagnosed after known gene analysis. Biallelic compound heterozygous variant of *SEMA3F* is narrowed down after variant prioritization using mouse deafness genes, in silico prediction tools, and minor allele frequencies (MAF) in Korean Variant Archive 2 (KOVA2). The KOVA2 and Rare Exome Variant Ensemble Learner (REVEL).

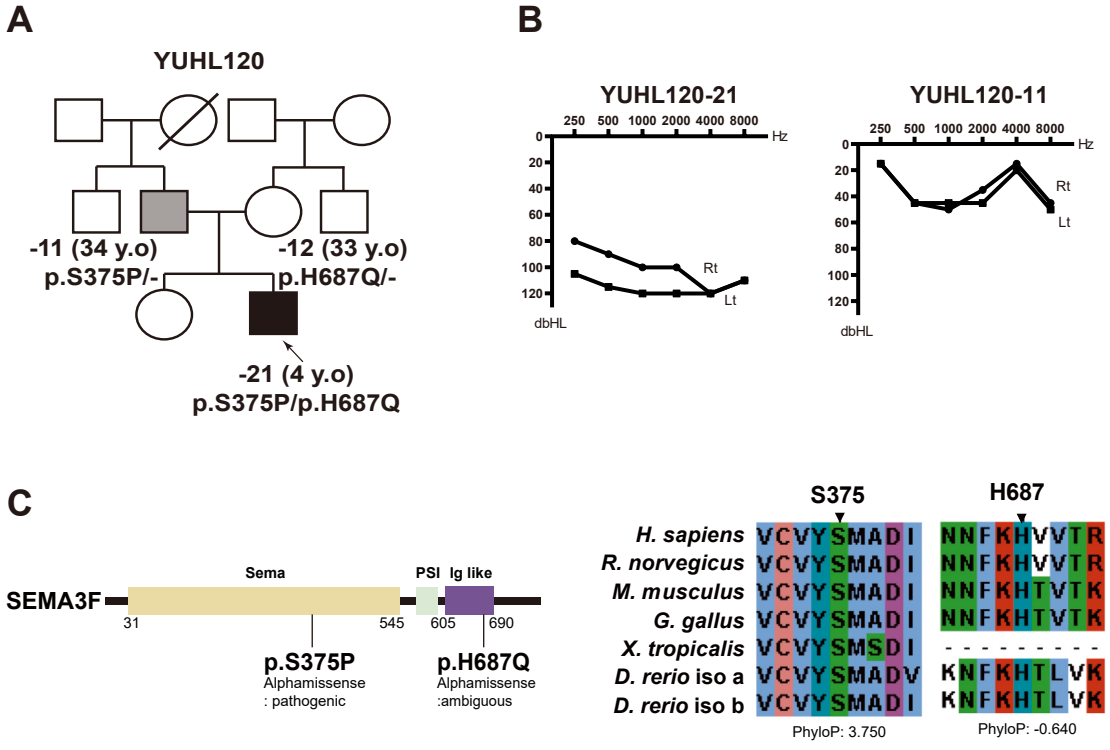

Fig. 3. Biallelic *SEMA3F* variants are detected in a proband with congenital hearing loss. (A) Pedigree of YUHL120 family in which the proband is identified with biallelic *SEMA3F* variants. The proband is indicated by using an arrow. Affected individual in the family with a different degree of hearing loss to the proband colored in gray. (B) Audiological phenotype of 2 affected individuals in YUHL120 family. (C) Summary of variant positions at SEMA3F domain and in silico prediction scores.

Table 1. Variants of *SEMA3F* identified in YUHL120-21

Sex	Age of onset	Chromosomal position (hg19)	Nucleotide change	Amino-acid change	Exon	dbSNP[a]	gnomAD v4 (POPMAX)[b]	KOVA2[c]	REVEL[d]	ACMG guideline[e]
M	Congenital	chr3:50220887_T/C	c.T1123C	p.Ser375Pro	12	rs1699093353	2.052-6e (2.003-5e; EAS)	-	0.565	VUS (PM2)
		chr3:50225251_C/A	c.C2061A	p.His687Gln	19	-	-	-	0.302	VUS (PM2)

KOVA2, Korean Variant Archive 2; REVEL, rare exome variant ensemble learner.
[a] dbSNP database (http://www.ncbi.nlm.nih.gov/SNP).
[b] gnomAD browser (http://exac.broadinstitute.org/).
[c] AF archived from KOVA2 (the Korean Variant Archive 2, approximately $n = 5,305$).
[d] Rare exome variant ensemble learner score predicting the deleteriousness of variants colored in red.
[e] PM2 is a criteria given when the MAF of variants are absent or in the range of AF < 0.0007.

contained 2 furin recognition motifs (KXRXRR), from residues 581 to 586 and from 774 to 779 (Fig. S3). Furin processing of the SEMA3F protein by a motif region of 774 to 779 residues is essential in the production of the mature C-terminal SEMA3F protein, which is required for direct physical interaction with the b1 domain of neuropilin (Parker et al., 2010). Plexin-neuropilin complexes are functional semaphorin receptors that mediate several semaphorin-related cellular events (Rohm et al., 2000), including repulsive signaling by SEMA3F and Nrp2, which inhibits type I neuronal innervation to OHCs. Reduction of processed SEMA3F protein may indicate the interfered binding of SEMA3F to its receptor complex mainly Nrp2.

The 2 variants might have different pathogenic mechanisms as they are located in different domains of SEMA3F. The p.Ser375Pro variant is located in the SEMA domain, which plays an important role in the dimerization of the SEMA3F protein (Alto and Terman, 2017). Immunoblotting revealed that the p.Ser375Pro variant reduced the dimerization of SEMA3F proteins, both in lysates and after secretion. A decrease in the functional dimer of SEMA3F proteins may result in the reduction of processed SEMA3F. The p.His687Gln variant located in the Ig domain did not affect the formation of the monomer and dimer SEMA3Fs. Because little is known about the role of the Ig domain, it is difficult to link the variant to the function of the domain. Nevertheless, p.His867Gln variant protein showed intervened furin processing, similar to that of the p.Ser375Pro protein, and failed to depolymerize the cytoskeletal structures of HUVECs.

The father of the proband (YUHL120-11) exhibited mild hearing loss characterized by a hearing loss of 26 to 45 dB, with onset later than that of the proband. The hearing loss of the father might be due to different genetic variants or possibly due to the deleterious combinations of a heterozygous *SEMA3F* variant with environmental factors. It is also known that loss of proper development of SGN is a key aspect of congenital and noise-induced hearing loss (Appler and Goodrich, 2011; Coate et al., 2015; Coate and Kelley, 2013; Fritzsch et al., 2004; Green et al., 2012). Additionally, the pLI score of SEMA3F is 1.0, indicating that the loss-of-function variants of *SEMA3F* are absent in the population database; therefore, the gene would be haploinsufficient. The variant identified in YUHL120-11 was p.Ser375Pro, which resulted in significantly reduced dimeric forms of SEMA3F in our functional studies and was, therefore, likely to contribute to a dosage-dependent trait. Therefore, the mild hearing loss of the father may suggest that partial deficiency of *SEMA3F* is also linked to autosomal-dominant hearing loss with late onset. To obtain reliable phenotype-genotype correlations, however, additional characterization of patients with *SEMA3F* variants would need to be identified.

Although SEMA3F is not associated with any other diseases in Online Mendelian Inheritance in Man (https://www.omim.org/), heterozygous loss-of-function variants of *SEMA3F*, including missense variants, have been linked to idiopathic hypogonadotropic hypogonadism, a disease characterized by absent puberty and subsequent infertility due to gonadotropin-releasing hormone deficiency (Kotan et al., 2021). However, the patient (YUHL120-21) and the father (YUHL120-11) with the p.Ser375Pro variant did not suffer from idiopathic hypogonadotropic hypogonadism, indicating its variable phenotype range.

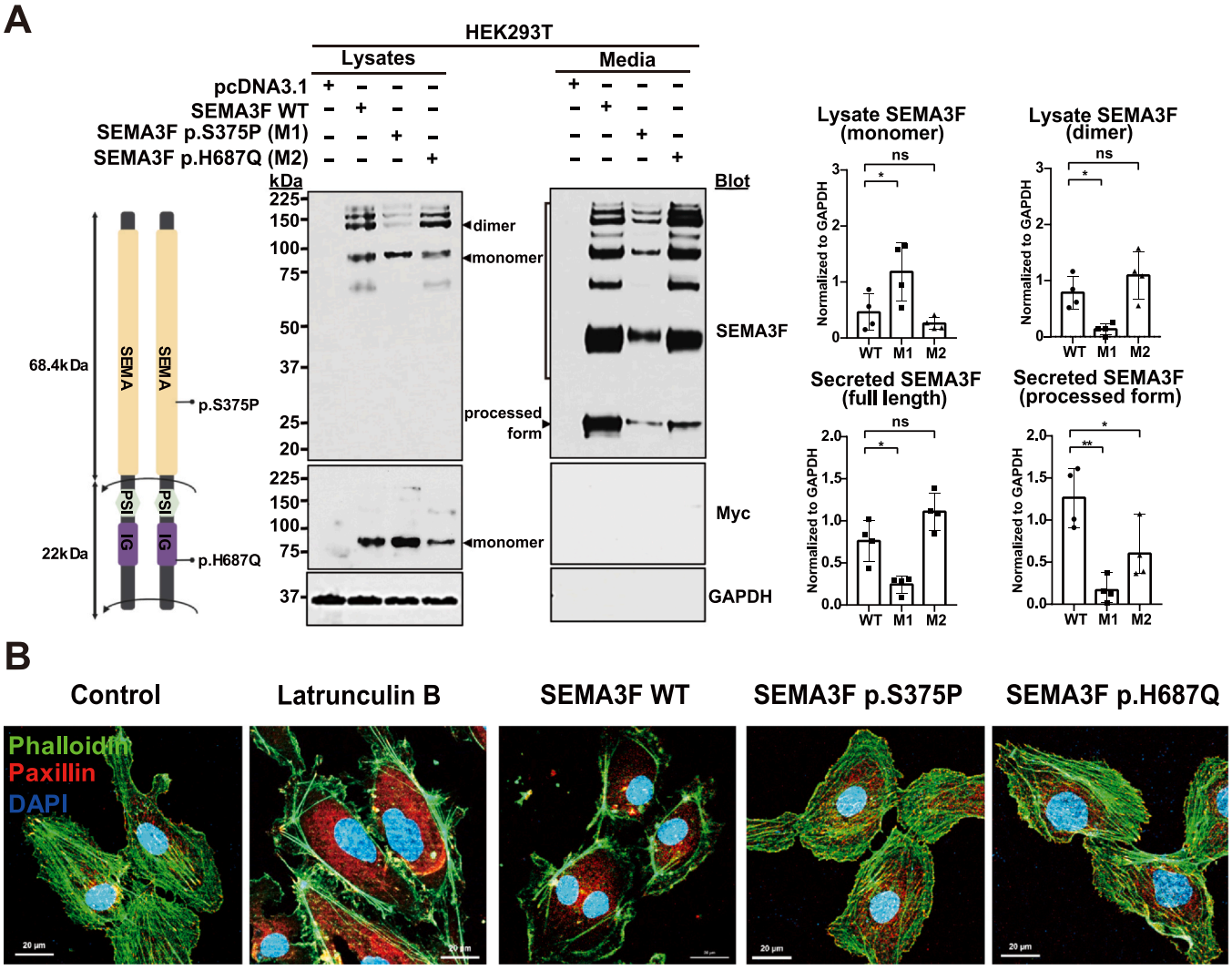

Fig. 4. Variants of *SEMA3F* are partial loss-of-function. (A) Expression and secretion profiles of wild-type and variant SEMA3F in HEK293T cells. (B) Immunofluorescence staining of HUVECs treated with culture media of cells overexpressing wild-type SEMA3F or variant SEMA3F variants. Control (nontreated HUVECs) and latrunculin B (HUVECs treated with chemical named latrunculin B, cell-contraction reagent) are shown as negative and positive controls, respectively. Statistical comparisons are performed using 2-way ANOVA with Bonferroni's correction for multiple comparisons (**P* < .05, ***P* < .01). n.s., nonsignificant.

In this study, we identified rare biallelic variants of *SEMA3F* as the genetic basis for nonsyndromic hearing loss, providing the first genetic evidence that links *SEMA3F* variants to hearing loss in humans. The identified missense variants significantly impair the ability of SEMA3F to depolymerize actin, resulting in a loss-of-function effect. Loss of SEMA3F expression in the murine inner ear is associated with various cochlear defects, particularly affecting the OHC region and SGN projections. These findings contribute to a deeper genetic understanding of hearing loss and shed light on potential therapeutic targets for interventions, particularly for hearing loss with rare genetic causes.

FUNDING AND SUPPORT

This work was supported by the National Research Foundation of Korea grants funded by the Korean government (RS-2023-00261905 to H.Y.G., 2022R1A2C3007281 to J. B., RS-2024-00346485 to J.J., and Mouse Disease Phenotyping Center RS-2024-00400118 to J.B. and H.Y.G.) and the Team Science Award of Yonsei University College of Medicine (6-2021-0002 to J.J., 6-2021-0003 to H.Y.G., and 6-2021-0004 to J.B.).

AUTHOR CONTRIBUTIONS

Lee Ho: Resources. **Seong Je Kyung:** Resources. **Kim Kyu Min:** Investigation. **Jung Jinsei:** Writing – review and editing, Supervision, Resources, Funding acquisition, Conceptualization. **Choi Jae Young:** Resources, Conceptualization. **Gee Heon Yung:** Writing – review and editing, Visualization, Supervision, Resources, Funding acquisition, Conceptualization. **Joo Sun Young:** Writing – original draft, Visualization, Validation, Methodology, Investigation, Formal analysis. **Bok Jinwoong:** Writing – review and editing, Visualization, Supervision, Resources, Funding acquisition, Conceptualization. **Kim Jung Ah:** Investigation, Formal analysis. **Min Hyehyun:** Writing – original draft, visualization, Validation, Investigation,

Formal analysis. **Jang Seung Hyun:** Investigation, Formal analysis. **Kim Se Jin:** Investigation, Formal analysis.

DECLARATION OF COMPETING INTERESTS

The authors declare that they have no known competing financial interests or personal relationships that could have appeared to influence the work reported in this paper.

DATA AVAILABILITY STATEMENT

The datasets generated during and/or analyzed during the current study are available from the corresponding author on request.

ACKNOWLEDGMENTS

We extend our sincere appreciation to the families that agreed to participate in this study. We also express our gratitude to the Yonsei Advanced Imaging Center. Bioresources or Korean population database for this study were provided by the National Biobank of Korea, Centers for Disease Control and Prevention, Republic of Korea (4845-301, 4851-302, and -307).

ORCID

Sun Young Joo https://orcid.org/0000-0001-8121-9714
Jinwoong Bok https://orcid.org/0000-0003-1958-1872
Heon Yung Gee https://orcid.org/0000-0002-8741-6177

APPENDIX A. SUPPLEMENTARY MATERIAL

Supplemental material associated with this article can be found online at: doi:10.1016/j.mocell.2025.100190.

Received September 24, 2024
Revised January 22, 2025
Accepted January 30, 2025
Available online 3 February 2025.

REFERENCES

Alto, L.T., and Terman, J.R. (2017). Semaphorins and their signaling mechanisms. Methods Mol Biol, *1493*, 1-25. https://doi.org/10.1007/978-1-4939-6448-2_1

Appler, J.M., and Goodrich, L.V. (2011). Connecting the ear to the brain: molecular mechanisms of auditory circuit assembly. Prog. Neurobiol. *93*, 488-508.

Bielenberg, D.R., Hida, Y., Shimizu, A., Kaipainen, A., Kreuter, M., Kim, C.C., and Klagsbrun, M. (2004). Semaphorin 3F, a chemorepulsant for endothelial cells, induces a poorly vascularized, encapsulated, nonmetastatic tumor phenotype. J. Clin. Invest. *114*, 1260-1271.

Bielenberg, D.R., Shimizu, A., and Klagsbrun, M. (2008). Semaphorin-induced cytoskeletal collapse and repulsion of endothelial cells. Methods Enzymol. *443*, 299-314.

Bowl, M.R., Simon, M.M., Ingham, N.J., Greenaway, S., Santos, L., Cater, H., Taylor, S., Mason, J., Kurbatova, N., Pearson, S., et al. (2017). A large scale hearing loss screen reveals an extensive unexplored genetic landscape for auditory dysfunction. Nat. Commun. *8*, 886.

Chang, M.Y., Kim, A.R., Kim, N.K., Lee, C., Lee, K.Y., Jeon, W.S., Koo, J.W., Oh, S.H., Park, W.Y., Kim, D., et al. (2015). Identification and clinical implications of novel MYO15A mutations in a non-consanguineous korean family by targeted exome sequencing. Mol. Cells, *38*, 781-788.

Cheng, J., Novati, G., Pan, J., Bycroft, C., Zemgulyte, A., Applebaum, T., Pritzel, A., Wong, L.H., Zielinski, M., Sargeant, T., et al. (2023). Accurate proteome-wide missense variant effect prediction with AlphaMissense. Science, *381*, Article eadg7492.

Chua, E.W., Ooi, J., and Nor Muhammad, N.A. (2024). A concise guide to essential R packages for analyses of DNA, RNA, and proteins. Mol. Cells, *47*, Article 100120.

Coate, T.M., and Kelley, M.W. (2013). Making connections in the inner ear: recent insights into the development of spiral ganglion neurons and their connectivity with sensory hair cells. Semin. Cell Dev. Biol. *24*, 460-469.

Coate, T.M., Spita, N.A., Zhang, K.D., Isgrig, K.T., and Kelley, M.W. (2015). Neuropilin-2/Semaphorin-3F-mediated repulsion promotes inner hair cell innervation by spiral ganglion neurons. Elife, *4*, e07830.

Collins, R.L., Brand, H., Karczewski, K.J., Zhao, X., Alfoldi, J., Francioli, L.C., Khera, A.V., Lowther, C., Gauthier, L.D., Wang, H., et al. (2021). Author correction: a structural variation reference for medical and population genetics. Nature, *590*, Article E55.

D'Aurizio, R., Pippucci, T., Tattini, L., Giusti, B., Pellegrini, M., and Magi, A. (2016). Enhanced copy number variants detection from whole-exome sequencing data using EXCAVATOR2. Nucleic Acids Res. *44*, Article e154.

Fritzsch, B., Tessarollo, L., Coppola, E., and Reichardt, L.F. (2004). Neurotrophins in the ear: their roles in sensory neuron survival and fiber guidance. Prog. Brain Res. *146*, 265-278.

Green, S.H., Bailey, E., Wang, Q., and Davis, R.L. (2012). The Trk A, B, C's of neurotrophins in the cochlea. Anat. Rec. *295*, 1877-1895.

Guttmann-Raviv, N., Shraga-Heled, N., Varshavsky, A., Guimaraes-Sternberg, C., Kessler, O., and Neufeld, G. (2007). Semaphorin-3A and semaphorin-3F work together to repel endothelial cells and to inhibit their survival by induction of apoptosis. J Biol. Chem. *282*, 26294-26305.

Ingham, N.J., Pearson, S.A., Vancollie, V.E., Rook, V., Lewis, M.A., Chen, J., Buniello, A., Martelletti, E., Preite, L., Lam, C.C., et al. (2019). Mouse screen reveals multiple new genes underlying mouse and human hearing loss. PLoS Biol. *17*, e3000194.

Jang, S.H., Yoon, K., and Gee, H.Y. (2024). Common genetic etiologies of sensorineural hearing loss in Koreans. Genomics Inform. *22*, 27.

Jung, J., Joo, S.Y., Min, H., Roh, J.W., Kim, K.A., Ma, J.H., Rim, J.H., Kim, J.A., Kim, S.J., Jang, S.H., et al. (2024). MYH1 deficiency disrupts outer hair cell electromotility, resulting in hearing loss. Exp. Mol. Med. *56*, 2423-2435.

Jung, J., Lee, J.S., Cho, K.J., Yu, S., Yoon, J.H., Yung Gee, H., and Choi, J.Y. (2017). Genetic predisposition to sporadic congenital hearing loss in a pediatric population. Sci. Rep. *7*, Article 45973.

Kikkawa, Y., Seki, Y., Okumura, K., Ohshiba, Y., Miyasaka, Y., Suzuki, S., Ozaki, M., Matsuoka, K., Noguchi, Y., and Yonekawa, H. (2012). Advantages of a mouse model for human hearing impairment. Exp. Anim. Tokyo, *61*, 85-98.

Kim, B.J., Oh, D.Y., Han, J.H., Oh, J., Kim, M.Y., Park, H.R., Seok, J., Cho, S.D., Lee, S.Y., Kim, Y., et al. (2020). Significant Mendelian genetic contribution to pediatric mild-to-moderate hearing loss and its comprehensive diagnostic approach. Genet. Med. *22*, 1119-1128.

Kim, J.A., Kim, S.H., Seo, J.S., Noh, H., Jeong, H., Kim, J., Jeon, D., Kim, J.J., On, D., Yoon, S., et al. (2022). Temporal transcriptome

analysis of SARS-CoV-2-infected lung and spleen in human ACE2-transgenic mice. Mol. Cells, *45*, 896-910.

Koh, Y.I., Oh, K.S., Kim, J.A., Noh, B., Choi, H.J., Joo, S.Y., Rim, J.H., Kim, H.Y., Kim, D.Y., Yu, S., et al. (2022). OSBPL2 mutations impair autophagy and lead to hearing loss, potentially remedied by rapamycin. Autophagy, *18*, 2593-2614.

Kotan, L.D., Ternier, G., Cakir, A.D., Emeksiz, H.C., Turan, I., Delpouve, G., Kardelen, A.D., Ozcabi, B., Isik, E., Mengen, E., et al. (2021). Loss-of-function variants in SEMA3F and PLXNA3 encoding semaphorin-3F and its receptor plexin-A3 respectively cause idiopathic hypogonadotropic hypogonadism. Genet. Med. *23*, 1008-1016.

Lee, J., Lee, J., Jeon, S., Lee, J., Jang, I., Yang, J.O., Park, S., Lee, B., Choi, J., Choi, B.O., et al. (2022). A database of 5305 healthy Korean individuals reveals genetic and clinical implications for an East Asian population. Exp. Mol. Med. *54*, 1862-1871.

Li, H. (2013). Aligning sequence reads, clone sequences and assembly contigs with BWA-MEM. arXiv preprint arXiv:1303.3997.

Ma, J.H., Lee, E., Yoon, S.H., Min, H., Oh, J.H., Hwang, I., Sung, Y., Ryu, J.H., Bok, J., and Yu, J.W. (2022). Therapeutic effect of NLRP3 inhibition on hearing loss induced by systemic inflammation in a CAPS-associated mouse model. EBioMedicine, *82*, Article 104184.

Oh, K.S., Roh, J.W., Joo, S.Y., Ryu, K., Kim, J.A., Kim, S.J., Jang, S.H., Koh, Y.I., Kim, D.H., Kim, H.Y., et al. (2023). Overlooked KCNQ4 variants augment the risk of hearing loss. Exp. Mol. Med. *55*, 844-859.

Ohyama, T., and Groves, A.K. (2004). Generation of Pax2–Cre mice by modification of a Pax2 bacterial artificial chromosome. genesis, *38*, 195-199.

Park, G., Kim, S.S., Shim, J., and Lee, S.-J.V. (2025). Brief guide to immunostaining. Mol. Cells, *48*, Article 100157.

Parker, M.W., Hellman, L.M., Xu, P., Fried, M.G., and Vander Kooi, C.W. (2010). Furin processing of semaphorin 3F determines its anti-angiogenic activity by regulating direct binding and competition for neuropilin. Biochemistry, *49*, 4068-4075.

Plagnol, V., Curtis, J., Epstein, M., Mok, K.Y., Stebbings, E., Grigoriadou, S., Wood, N.W., Hambleton, S., Burns, S.O., Thrasher, A.J., et al. (2012). A robust model for read count data in exome sequencing experiments and implications for copy number variant calling. Bioinformatics, *28*, 2747-2754.

Poplin, R., Ruano-Rubio, V., DePristo, M.A., Fennell, T.J., Carneiro, M. O., Van der Auwera, G.A., Kling, D.E., Gauthier, L.D., Levy-Moonshine, A., and Roazen, D. (2017). Scaling accurate genetic variant discovery to tens of thousands of samples. bioRxiv, 201178.

Regano, D., Visintin, A., Clapero, F., Bussolino, F., Valdembri, D., Maione, F., Serini, G., and Giraudo, E. (2017). Sema3F (Semaphorin 3F) selectively drives an extraembryonic proangiogenic program. Arterioscler. Thromb. Vasc. Biol. *37*, 1710-1721.

Rim, J.H., Lee, J.S., Jung, J., Lee, J.H., Lee, S.-T., Choi, J.R., Choi, J.Y., Lee, M.G., and Gee, H.Y. (2019). Systematic evaluation of gene variants linked to hearing loss based on allele frequency threshold and filtering allele frequency. Sci. Rep. *9*, 4583.

Rim, J.H., Noh, B., Koh, Y.I., Joo, S.Y., Oh, K.S., Kim, K., Kim, J.A., Kim, D.H., Kim, H.Y., Yoo, J.E., et al. (2022). Differential genetic diagnoses of adult post-lingual hearing loss according to the audiogram pattern and novel candidate gene evaluation. Hum. Genet. *141*, 915-927.

Rohm, B., Ottemeyer, A., Lohrum, M., and Puschel, A.W. (2000). Plexin/neuropilin complexes mediate repulsion by the axonal guidance signal semaphorin 3A. Mech. Dev. *93*, 95-104.

Shearer, A.E., Hildebrand, M.S., Odell, A.M., and Smith, R.J.H. (1999). Genetic Hearing Loss Overview. In GeneReviews®, M.P. Adam,, ed. *(Seattle: University of Washington).*

Shimizu, A., Mammoto, A., Italiano, J.E., Jr., Pravda, E., Dudley, A.C., Ingber, D.E., and Klagsbrun, M. (2008). ABL2/ARG tyrosine kinase mediates SEMA3F-induced RhoA inactivation and cytoskeleton collapse in human glioma cells. J. Biol. Chem. *283*, 27230-27238.

Shin, D.H., Jung, J., Koh, Y.I., Rim, J.H., Lee, J.S., Choi, H.J., Joo, S.Y., Yu, S., Cha, D.H., Lee, S.Y., et al. (2019). A recurrent mutation in KCNQ4 in Korean families with nonsyndromic hearing loss and rescue of the channel activity by KCNQ activators. Hum. Mutat. *40*, 335-346.

Sloan-Heggen, C.M., Bierer, A.O., Shearer, A.E., Kolbe, D.L., Nishimura, C.J., Frees, K.L., Ephraim, S.S., Shibata, S.B., Booth, K.T., Campbell, C.A., et al. (2016). Comprehensive genetic testing in the clinical evaluation of 1119 patients with hearing loss. Hum. Genet. *135*, 441-450.

Son, E.J., Ma, J.H., Ankamreddy, H., Shin, J.O., Choi, J.Y., Wu, D.K., and Bok, J. (2015). Conserved role of Sonic Hedgehog in tonotopic organization of the avian basilar papilla and mammalian cochlea. Proc. Natl. Acad. Sci. U.S.A. *112*, 3746-3751.

Toledano, S., Nir-Zvi, I., Engelman, R., Kessler, O., and Neufeld, G. (2019). Class-3 semaphorins and their receptors: potent multifunctional modulators of tumor progression. Int. J. Mol. Sci. *20*.

Van der Auwera, G.A., Carneiro, M.O., Hartl, C., Poplin, R., Del Angel, G., Levy-Moonshine, A., Jordan, T., Shakir, K., Roazen, D., and Thibault, J. (2013). From FastQ data to high-confidence variant calls: the genome analysis toolkit best practices pipeline. Curr. Protoc. Bioinformatics, *43* 11.10. 11-11.10. 33.

Walz, A., Feinstein, P., Khan, M., and Mombaerts, P. (2007). Axonal wiring of guanylate cyclase-D-expressing olfactory neurons is dependent on neuropilin 2 and semaphorin 3F. Development, *134*, 4063-4072.

Wu, T., Hu, E., Xu, S., Chen, M., Guo, P., Dai, Z., Feng, T., Zhou, L., Tang, W., Zhan, L., et al. (2021). clusterProfiler 4.0: a universal enrichment tool for interpreting omics data. Innovation, *2*, Article 100141.

Yu, S., Choi, H.J., Lee, J.S., Lee, H.J., Rim, J.H., Choi, J.Y., Gee, H.Y., and Jung, J. (2019). A novel early truncation mutation in OTOG causes prelingual mild hearing loss without vestibular dysfunction. Eur. J. Med. Genet. *62*, 81-84.

Zhong, L.X., Kun, S., Jing, Q., Jing, C., and Denise, Y. (2013). Non-syndromic hearing loss and high-throughput strategies to decipher its genetic heterogeneity. J. Otol. *8*, 6-24.